

Electronic Supplementary Information

Novel Dual Spectral Conversion via Eu^{2+} , Cu^+ -coactivated Core-Shell-Structured $\text{CaS}@\text{CaZnOS}$ Phosphors for Efficient Photosynthesis of Plants

Liu Yan,^a Mei Peng,^a Zirong Song,^a Yue He,^a Yulin Fan,^a Yuya Wang,^a Rumeng Xiong,^a Shixun Lian,^{a,b,*} Xinxian Ma,^{b,*} Zhongxian Qiu^{a,*}

*E-mail: sxlian@hunnu.edu.cn; maxinxian@163.com; zxqiu@hunnu.edu.cn.

a) Key Laboratory of Light-Energy Conversion Materials of Hunan Province College; College of Chemistry and Chemical Engineering, Hunan Normal University, Changsha, Hunan 410081, People's Republic of China.

b) College of Chemistry and Chemical Engineering, Ningxia Normal University, Guyuan, Gansu 756000, People's Republic of China.

S1. The concentration of Eu^{2+} on the effect of luminescence properties in red $\text{CaS}:\text{x}\text{Eu}^{2+}$ phosphors and $\text{CaS}:\text{x}\text{Eu}^{2+}, 10\%\text{Br}^-$ phosphors

$\text{CaS}:\text{Eu}$ and $\text{CaS}:\text{Eu},\text{Br}$ phosphors emit broadband red light at 650 nm under UV and green light excitation. In addition, the halide additives lead to an enlargement of the grain size and the gathering of particles. Br^- ions are introduced by adding a cosolvent CaBr_2 , and Br^- substitutes for S^{2-} , to enhance the luminescence intensity of the phosphors.^{1, 2} The ideal Eu^{2+} concentration in $\text{CaS}:\text{x}\%\text{Eu}^{2+}$ and $\text{CaS}:\text{x}\%\text{Eu}^{2+}, 10\%\text{Br}^-$ was determined to be 0.15% by experimental studies.

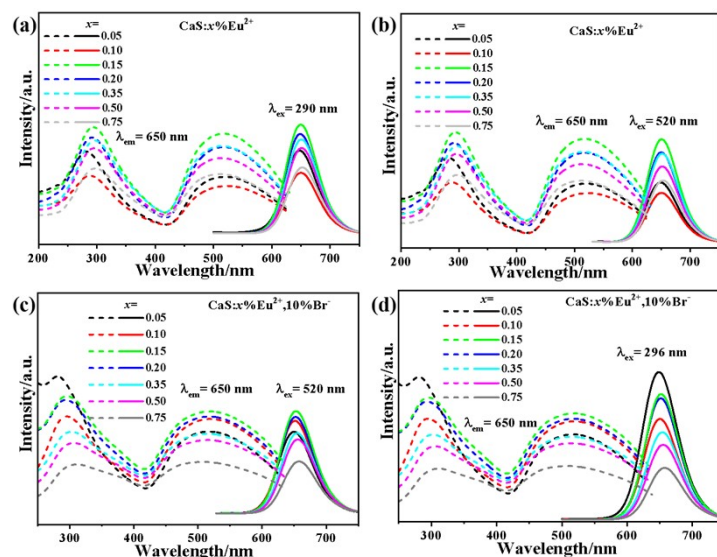


Figure S1. Photoluminescence spectra of $\text{CaS}:\text{x}\%\text{Eu}^{2+}$ (a) $\lambda_{\text{ex}}=290$ nm, $\lambda_{\text{em}}=650$ nm; (b) $\lambda_{\text{ex}}=520$ nm, $\lambda_{\text{em}}=650$ nm; Photoluminescence spectra of $\text{CaS}:\text{x}\%\text{Eu}^{2+}, 10\%\text{Br}^-$ (c) $\lambda_{\text{ex}}=520$ nm, $\lambda_{\text{em}}=650$ nm; (d) $\lambda_{\text{ex}}=296$ nm, $\lambda_{\text{em}}=650$ nm.

S2. The concentration of Cu^+ on the effect of luminescence properties in

CaS:yCu⁺,10%Br⁻ phosphors

Figure S2 shows the excitation (PLE) and emission spectra (PL) of the phosphor CaS:x%Cu⁺,10%Br⁻ (x=0.10-0.75). The plots in (a) and (b) show the dotted line curves of luminescence intensity and emission peaks with concentration. The Figures show the excitation spectrum when monitored at 314 nm and the emission spectrum when excited at a wavelength of 417 nm. The results show that all phosphors exhibit the characteristic Cu⁺ excitation and emission bands. As can be seen in (a), the phosphor has only one excitation band, with the excitation peak occurring in the UV region between 314±2 nm, as the transition from the ¹A_{1g}→¹E_g energy state of the Cu⁺ ion.^{3,4}

The results show that the phosphor can be effectively excited by UV light, and an emission band with a central wavelength in the blue region in the range of 427±12 nm is observed. This emission band is due to the 3d⁹4s→3d¹⁰ energy level transition of Cu⁺ ions during this process. As shown in Figures S2(a) and S2(b), the emission intensity of the phosphor in the blue region first increases with increasing Cu⁺ ion concentration and then decreases to peak at x=0.15. The peak emission wavelength shifts to the long wavelength direction with the increase of Cu⁺ content, since Cu⁺ has a 3d¹⁰ electron configuration and the d-electron level is very sensitive to the surrounding crystal field. Since d-electrons are involved in the luminescence of Cu⁺, the surrounding crystal field changes with the d-electron interaction of Cu⁺, resulting in different peak emission wavelengths (as shown in Figure. S2c and Figure. S2d).

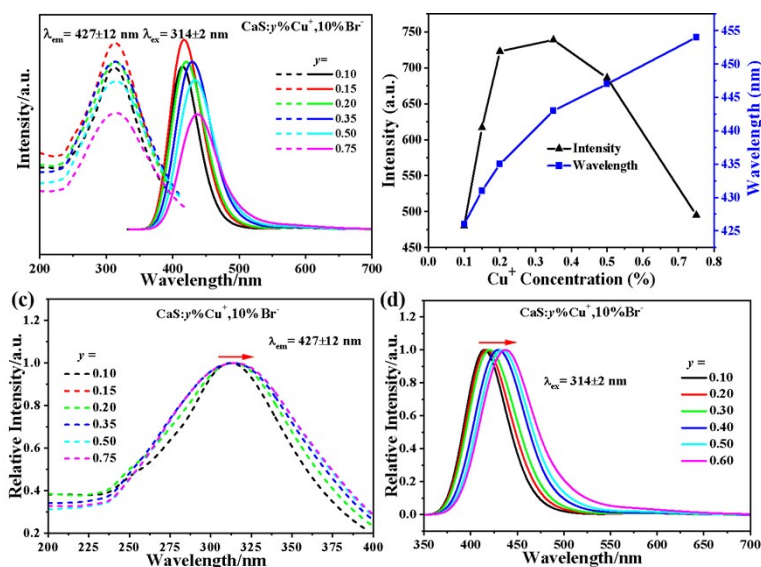


Figure S2. Photoluminescence spectra of CaS:x%Cu⁺,10%Br⁻ (a) $\lambda_{ex} = 314\pm 2$ nm, $\lambda_{em} = 427\pm 12$ nm; (b) dotted line plot of relative intensities corresponding to wavelength and emission intensity.

S3. Investigate the optimal concentration of Eu²⁺, Cu⁺ in CaS: Eu²⁺, Cu⁺ and CaS:Eu²⁺,Cu⁺,Br⁻ phosphors

Figures S3(a-d) below show the excitation spectra (PLE), emission spectra (PL), and dotted lines of emission of blue light under UV excitation and emission of red light under green excitation of CaS:0.15%Eu²⁺,x%Cu⁺,10%Br⁻ phosphor. As shown in Figures S3(a), and (d), the red-light emission at ~644 nm under 455 nm excitation is due to the 4f⁶5d→⁸S_{7/2} (4f⁷) transition of Eu²⁺, and the excitation band under 644 monitoring is a large broad excitation band attributed to the 4f⁷→4f⁶5d transition of Eu²⁺. The intensity of the red luminescence first increases and then decreases with the concentration of Cu⁺ ions, peaking at a concentration of 0.05%.

The peak in the excitation band at 309 nm under 410 nm monitoring in Figures. S3(b-d) is attributable to the ¹A_{1g}→¹E_g transition of Cu⁺. The blue light at ~410 nm and red light at ~644 nm emitted upon excitation of 309 nm

is due to the $3d^{10} \rightarrow 3d^9 4s$ transition of Cu^+ and the $4f^6 5d \rightarrow {}^8S_{7/2}$ transition of Eu^{2+} , respectively. According to Figure S3(d), the intensity of red luminescence increases with increasing Cu^+ ion concentration, and peaks at 0.15%, while the intensity of blue luminescence first increases and then decreases at an optimum concentration of 0.35%.

The excitation spectra (PLE) and emission spectra (PL) of $\text{CaS}:0.15\% \text{Eu}^{2+}, x\% \text{Cu}^+, 10\% \text{Br}^-$ phosphor are shown in Figure S3(e-g) below. The results show that the characteristic spectrum of $\text{CaS}:0.15\% \text{Eu}^{2+}, x\% \text{Cu}^+, 10\% \text{Br}^-$ is an excitation band with a peak of 303 nm obtained at 406 nm monitoring and is mainly attributed to the ${}^1A_{1g} \rightarrow {}^1E_g$ transition of Cu^+ and the emission of blue and red light, respectively, at 303 nm excitation by the energy conversion of band edge transition absorption and the $4f^6 5d \rightarrow {}^8S_{7/2}$ transition of Eu^{2+} . Figures S3(e) and S3(g) show how the intensity of the blue light emitted from the phosphor gradually decreases as the concentration of Eu^{2+} ions increases. This is because the Cu^+ emission band and the Eu^{2+} excitation band partially overlap. The energy transfer between Cu^+ and Eu^{2+} is indicated by a decrease in blue light intensity and an increase in red light intensity during UV excitation. The intensity of the red light increases with Eu^{2+} concentration, and peaks at $y=0.05$.

As shown in Figures S3(f) and S3(g), the red light emitted at 455 nm is due to the $4f^6 5d \rightarrow {}^8S_{7/2}$ ($4f^7$) transition of Eu^{2+} ~ 644 nm, and the excitation band at 647 nm is a large, broad excitation band attributed to the $4f^7 \rightarrow 4f^6 5d$ transition of Eu^{2+} . As the Eu^{2+} ion concentration increases, the intensity of the red luminescence increases and then decreases. The best intensity is achieved at a Eu^{2+} concentration of 0.10%.

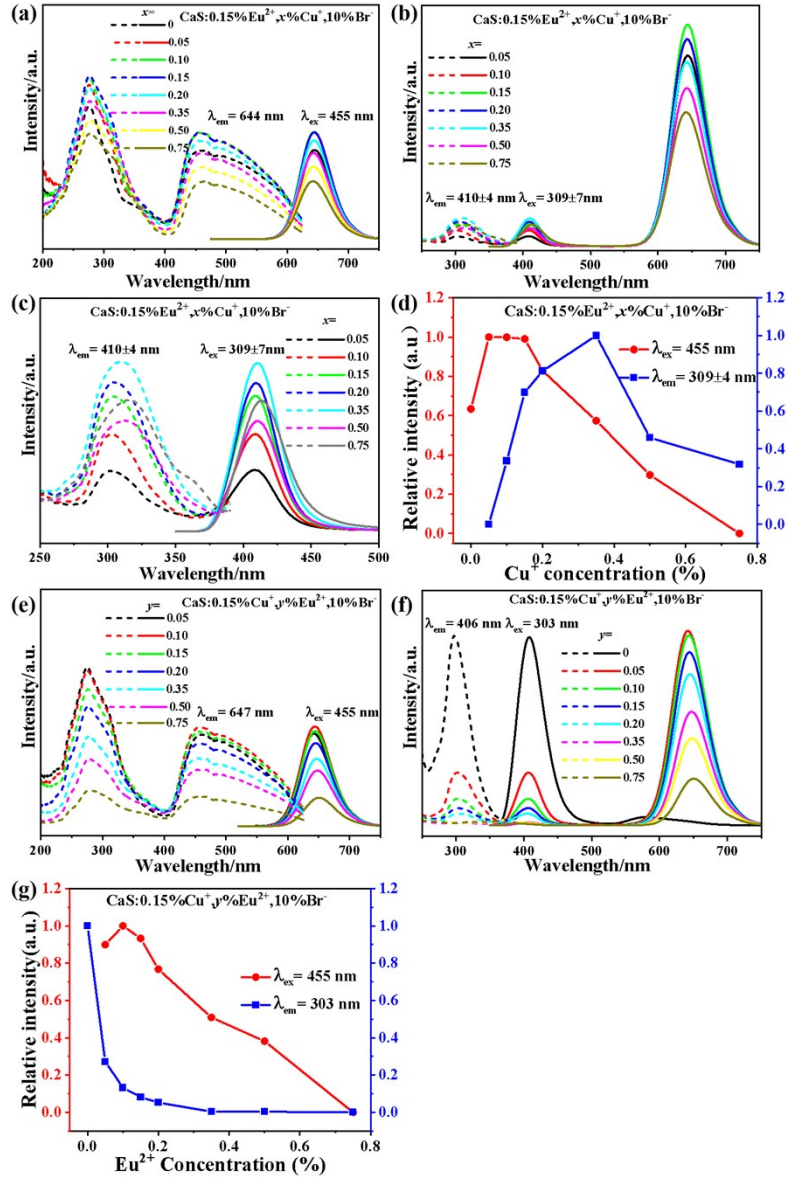


Figure S3. Photoluminescence spectra of $\text{CaS:0.15\%Eu}^{2+},x\%\text{Cu}^+,10\%\text{Br}^-$ (a) $\lambda_{\text{ex}} = 455 \text{ nm}$, $\lambda_{\text{em}} = 644 \text{ nm}$; (b) $\lambda_{\text{ex}} = 309 \pm 7 \text{ nm}$, $\lambda_{\text{em}} = 410 \pm 4 \text{ nm}$; (c) a magnified view of figure (b); (d) dotted line plot of relative intensities corresponding to red and blue emission. Photoluminescence spectra of $\text{CaS:0.15\%Cu}^+,y\%\text{Eu}^{2+},10\%\text{Br}^-$ (e) $\lambda_{\text{ex}} = 303 \text{ nm}$, $\lambda_{\text{em}} = 406 \text{ nm}$; (f) $\lambda_{\text{ex}} = 309 \pm 7 \text{ nm}$, $\lambda_{\text{em}} = 410 \pm 4 \text{ nm}$; (g) Dotted line plot of relative intensities corresponding to red-blue emission.

S4. Investigate the optimal concentration of Cu^+ in CaZnOS:x\%Cu^+ and $\text{CaZnOS:x\%Cu}^+,2\%\text{Br}^-$

The excitation and emission spectra of CaZnOS:Cu^+ and $\text{CaZnOS:Cu}^+,\text{Br}^-$ are displayed in Figures S4 (a) and (b), respectively. The intrinsic defect of CaZnOS reported in the literature is consistent with a broadband peak with a peak of $\sim 499 \text{ nm}$ in the green region at $x=0$, under excitation at $\sim 375 \text{ nm}$ (where the intrinsic point defect acts as the luminescent energy level to generate $\text{V}_2^+ \text{O} \rightarrow \text{V}_0 \text{O}$, resulting in luminescence)⁵. Consequently, the emission peak at $\sim 499 \text{ nm}$ is attributed to the intrinsic defect of CaZnOS . Following Cu^+ doping, the excitation spectra of CaZnOS:x\%Cu^+ were examined under 450 nm monitoring, as shown in Figure S4 (a). The excitation band includes a strong excitation band of $250\text{-}350 \text{ nm}$ and a weak excitation band of $350\text{-}400 \text{ nm}$, with the maximum peaks

located at ~ 332 nm and ~ 375 nm, respectively. This is due to the characteristic excitation transition of Cu^+ from $3d^{10}$ to $3d^94s$ and matrix absorption. Moreover, the material exhibits an emission peak at ~ 398 nm and ~ 450 nm, respectively, under 332 nm excitation. The energy level transition of Cu^+ in $\text{CaZnOS}:\text{Cu}$ is shown by the blue emission peak at 450 nm. According to relevant literature reports,⁶ the emission peak at 398 nm is attributed to the intrinsic defects of ZnO and a specific amount of Cu enters the ZnO lattice. Increases the possibility of free exciton states in the ZnO band structure, thereby increasing the exciton intensity of ultraviolet emission. On the other hand, the improvement of the defect structure reduces the deformation of the ZnO lattice, thereby enhancing the luminescence intensity of violet light emission. As the Cu content increased, the positions of the violet peaks did not shift considerably but the intensity of the violet peaks varied appreciably. The reduction observed in the luminescence intensity of violet peaks at 0.05% results from the diminution in the number of electron-hole pair recombinations due to the transfer of photoexcited electrons from ZnO to Cu ions. The reason for the existence of ZnO may be that during the high-temperature calcining process, the CaZnOS formed decomposes to produce ZnO, which remains on the surface of the sample. Figure S4(b) illustrates how the addition of CaBr_2 causes the emission band in the blue region to become much stronger than the emission band in the green region when Cu^+ is added. This results in an asymmetric broadband emission peak that forms and obscures the intrinsic emission band of the CaZnOS matrix, which is located at ~ 499 nm. Among them, the CaBr_2 additive can lead to an increase in grain size and particle aggregation, and usually, an increase in particle size plays a positive role in improving the luminescence intensity of solid phosphors. Furthermore, Br^- takes the place of S^{2-} and CaBr_2 serves as a co-solvent. We think that adding Br^- to the S^{2-} lattice contributes to luminescence enhancement, and that the melting impact of CaBr_2 is more important in generating a considerable increase in luminescence intensity. The blue emission intensity of $\text{CaZnOS}:\text{Cu},\text{Br}$ has therefore considerably risen as compared to Figure S4(a, b), suggesting that it is a phosphor that exhibits UV excitation and blue emission.

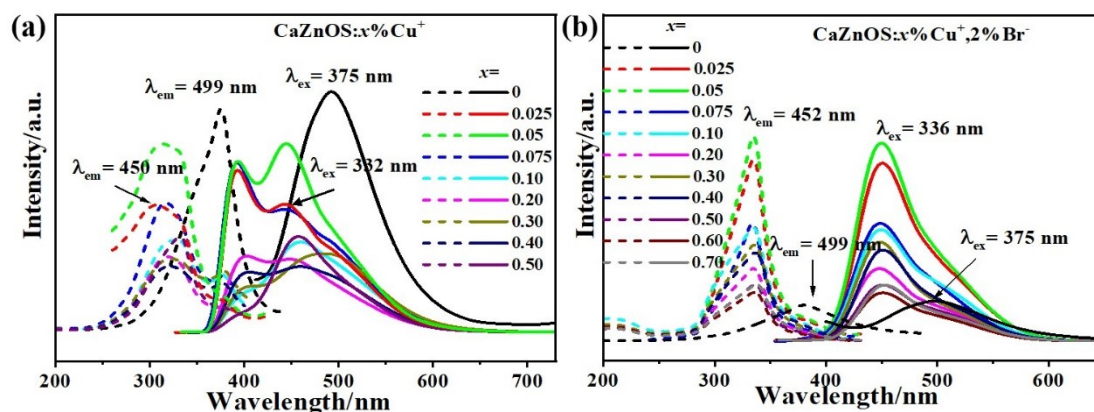


Figure S4. Photoluminescence spectra of $\text{CaZnOS}:x\%\text{Cu}^+$ (a) $\lambda_{\text{ex}} = 375$ nm, $\lambda_{\text{em}} = 499$ nm; $\lambda_{\text{ex}} = 332$ nm, $\lambda_{\text{em}} = 450$ nm; photoluminescence spectra of $\text{CaZnOS}:x\%\text{Cu}^+,2\%\text{Br}^-$ (b) $\lambda_{\text{ex}} = 375$ nm, $\lambda_{\text{em}} = 499$ nm; $\lambda_{\text{ex}} = 336$ nm, $\lambda_{\text{em}} = 452$ nm.

S5. The concentration of Cu^+ on the effect of luminescence properties in $\text{CaS}:\text{Eu}^{2+},\text{Cu}^+, \text{Br}^- @ \text{CaZnOS}:x\%\text{Cu}^+,2\%\text{Br}^-$ phosphors

The photoluminescence spectra of $\text{CaS}:\text{Cu}^+, \text{Eu}^{2+}, \text{Br}^- @ \text{CaZnOS}:x\%\text{Cu}^+,2\%\text{Br}^-$ are shown in Figure S5(a-c). The results show a peak at ~ 336 nm excitation band under 435 nm monitoring attributed to the $^1A_{1g} \rightarrow ^1T_{2g}$ transition of Cu^+ . The blue light at ~ 435 nm and the red light at 646 nm emitted at the 336 nm excitation are attributed to the $3d^{10} \rightarrow 3d^94s$ transition of Cu^+ and the $4f^65d \rightarrow 4f^7$ transition of Eu^{2+} , respectively. The best luminescence intensity is

obtained at a Cu^+ concentration of 0.05%, as shown in Figures S5(a) and S5(c), which also show that the blue luminescence intensity increases with the increase of Cu^+ ion concentration and then decreases.

Figures S5(b) and S5(c) show the luminescence of phosphor $\text{CaS:Eu}^{2+},\text{Cu}^+,\text{Br}^-@ \text{CaZnOS}:x\% \text{Cu}^+,2\% \text{Br}^-$ derived from the luminescence of CaS:Eu , with the dashed line representing the excitation band and the solid line representing the emission band. The red light emitted at 646 nm under 528 nm excitation is due to the $4f^65d \rightarrow ^8S_{7/2} (4f^7)$ transition of Eu^{2+} , and the excitation band under 646 nm monitoring is a large, broad excitation band attributed to the $4f^7 \rightarrow 4f^65d$ transition of Eu^{2+} . The intensity of red luminescence gradually decreases as the Eu^{2+} ion concentration increases. The intensity of blue light emission from the phosphor increases and subsequently decreases as the Cu^+ ion concentration rises, which is due to a partial overlap between the emission band of Cu^+ and the excitation band of Eu^{2+} . The intensity of red light decreases, blue light intensity increases, and then decreases under UV excitation, showing that energy is transferred between Cu^+ and Eu^{2+} . This could also explain why the intensity of the red light decreases linearly with concentration when the co-solvent CaBr_2 is also added to the CaZnOS:Cu shell. When monitored at 435 ± 5 nm, the excitation spectrum of the phosphor appeared asymmetric, which was significantly different from that of CaS:Cu (Figure S2) and CaZnOS:Cu (Figure S4). Subsequently, the photoluminescence spectrum of the phosphor powder with the best light intensity was subjected to Gaussian fitting (see Figures S5c and S5d), and three excitation and three emission peaks were obtained, which showed CaS:Cu ($\lambda_{\text{ex}}=310$ nm, $\lambda_{\text{em}}=420$ nm), CaZnOS:Cu ($\lambda_{\text{ex}}=334$ nm, $\lambda_{\text{em}}=451$ nm), CaZnOS ($\lambda_{\text{ex}}=376$ nm, $\lambda_{\text{em}}=500$ nm), the blue light emission is the luminescence superposition of core CaS:Cu and CaZnOS:Cu , it is a mixed light of two VTBs.

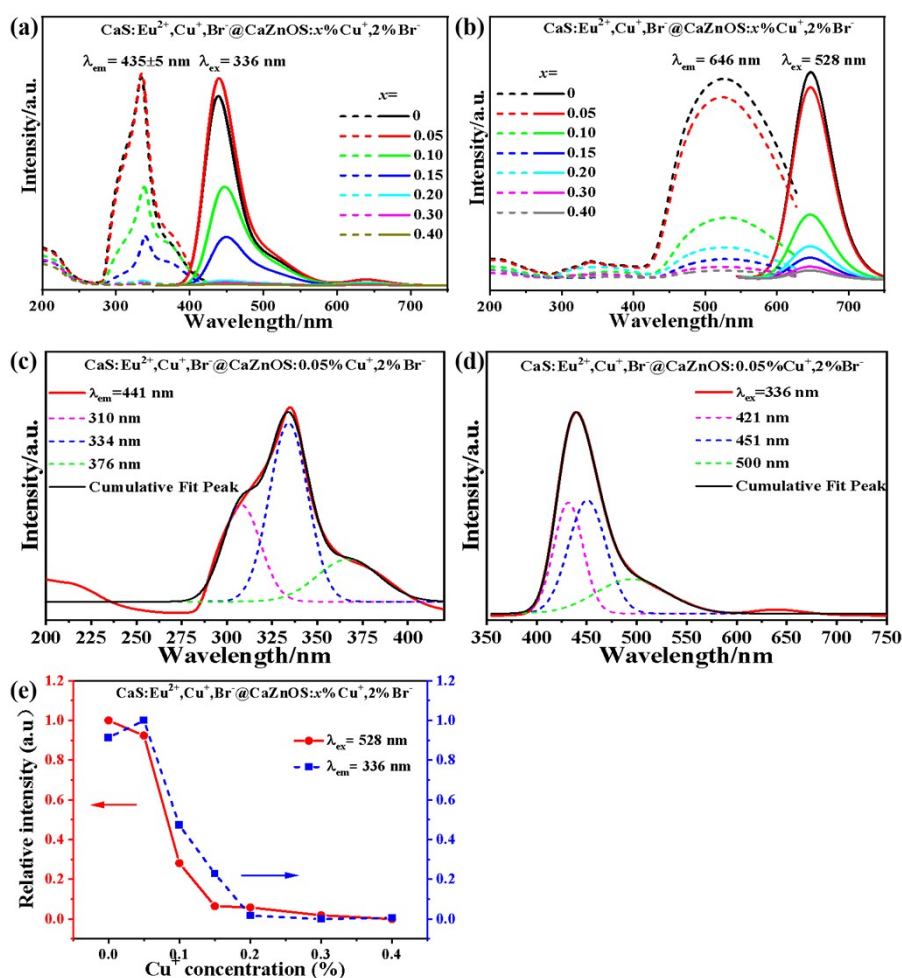


Figure S5. Photoluminescence spectra of $\text{CaS:Eu}^{2+},\text{Cu}^+,\text{Br}^-@ \text{CaZnOS}:x\% \text{Cu}^+,2\% \text{Br}^-$ (a) $\lambda_{\text{ex}}=336$ nm, $\lambda_{\text{em}}=435 \pm 5$ nm; (b) $\lambda_{\text{ex}}=528$ nm, $\lambda_{\text{em}}=646$ nm; (c) and (d) are the excitation and emission spectra after Gaussian fitting when $x=0.05$;

(e) dashed line of relative intensities corresponding to red and blue emission.

S6. The quantum efficiencies of the four phosphors at different wavelength excitations

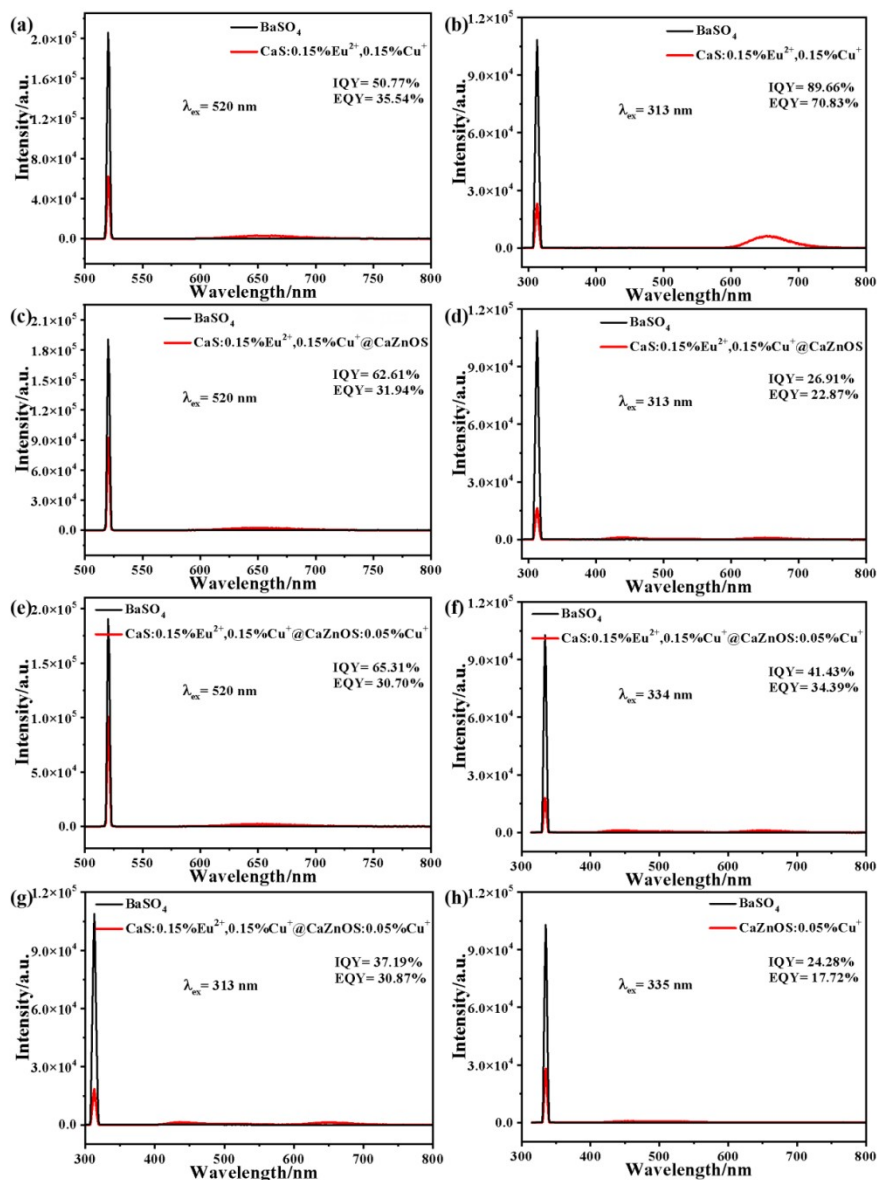


Figure S6. Luminescent spectra for QY measurement of CaS:Eu²⁺,Cu⁺,Br phosphors (a) λ_{ex} =520 nm, (b) λ_{ex} =313 nm; CaS:Eu²⁺,Cu⁺,Br@CaZnOS phosphor (c) λ_{ex} =520 nm, (d) λ_{ex} =313 nm; CaS:Eu²⁺,Cu⁺,Br@CaZnOS:0.05%Cu⁺ phosphor (e) λ_{ex} =520 nm, (f) λ_{ex} =334 nm, (g) λ_{ex} =313 nm; CaZnOS:0.05%Cu⁺ phosphor (h) λ_{ex} =334 nm.

References

1. T. Luo; Y. Du; Z. Qiu; Y. Li; X. Wang; W. Zhou; J. Zhang; L. Yu; S. Lian, Remarkably Enhancing Green-Excitation Efficiency for Solar Energy Utilization: Red Phosphors $\text{Ba}_2\text{ZnS}_3\text{:Eu}^{2+},\text{X}^-$ Co-Doped Halide Ions (X =Cl, Br, I). *Inorg. Chem.* 2017, **56**, 5720-5727.
2. X. Wang; J. Ke; Y. Wang; Y. Liang; J. He; Z. Song; S. Lian; Z. Qiu, One-Step Design of a Water-Resistant Green-to-Red Phosphor for Horticultural Sunlight Conversion. *ACS Agric. Sci. Technol.* 2021, **1**, 55-63.
3. S. Lian; C. Rong; D. Yin; S. Liu, Enhancing Solar Energy Conversion Efficiency: A Tunable Dual-Excitation Dual-Emission Phosphors and Time-Dependent Density Functional Theory Study. *J. Phys. Chem. C* 2009, **113**, 6298-6302.
4. X. Tong; J. Yang; P. Wu; X. Zhang; H. Seo, Color tunable emission from $\text{CaS:Cu}^+,\text{Mn}^{2+}$ rare-earth-free phosphors prepared by a simple carbon-thermal reduction method. *J. Alloy. Compd.* 2019, **779**, 399-403.
5. C. Pan; J. Zhang; M. Zhang; X. Yan; Y. Long; X. Wang, Intrinsic oxygen vacancies mediated multi-mechano-responsive piezoluminescence in undoped zinc calcium oxysulfide [J]. *Applied Physics Letters*, 2017, **110** (23): 233904
6. G. R. Khan, Optical band gap engineering of ZnO nanophosphors via Cu incorporation for ultraviolet–violet LED. *The European Physical Journal Plus* 2020, **135** (8), 684.